Hindawi
Journal of Nanomaterials
Volume 2020, Article ID 6173867, 7 pages
https://doi.org/10.1155/2020/6173867

Research Article

Hydrothermal Synthesis of Hydroxyapatite Assisted by Gemini Cationic Surfactant

Tao Zhang[1] **and Xiufeng Xiao**[2]

[1]*Department of Orthopedics Institute, Fuzhou Second Hospital Affiliated to Xiamen University, Fuzhou 350007, China*
[2]*Fujian Provincial Key Laboratory of Advanced Materials Oriented Chemical Engineering, College of Chemistry and Materials Science, Fujian Normal University, Fuzhou 350007, China*

Correspondence should be addressed to Xiufeng Xiao; xfxiao@fjnu.edu.cn

Received 1 February 2020; Revised 6 June 2020; Accepted 26 June 2020; Published 15 July 2020

Academic Editor: Zhi Li Xiao

Hydroxyapatite (HAp) has been synthesized by a hydrothermal treatment in the presence of a Gemini cationic surfactant. This process is a new strategy of synthesis and mainly consists of two parts, i.e., an ordinary hydrothermal treatment and a liquid-solid-solution reaction (LSS strategy). Crystalline HAp nanorods or nanogranules with length of 50-180 nm and width of 30-40 nm were produced by ordinary hydrothermal treatment. By contrary, HAp spheres with a 3D architecture were fabricated with Gemini cationic surfactant by LSS strategy. For Gemini cationic surfactant concentration of 0.05%, spherical HAp particles with an average diameter of 1.7 μm were obtained.

1. Introduction

Hydrothermal method, a common way to prepare HAp, involves chemical reactions occurring in an aqueous solution at high temperature and pressure. The hydrothermal method could be considered as a chemical precipitation method in which the aging process is carried on inside an autoclave or pressure vessel [1]. It has been proved that HAp nanorods obtained by the hydrothermal method are highly crystalline and stoichiometric [2]. The purity and Ca/P of HAp sharply increased with hydrothermal temperature [3].

It was difficult to control the shape, size, and size distribution of nanoparticles prepared by the hydrothermal method. To overcome this drawback, the use of organic modifiers or surfactants was proposed. Jiang et al. proposed a soft way for the preparation of HAp of different shapes by using a combination of Na_2EDTA and citric acid (CA) at pH = 3.60 [4]. CA was selected due to its selective adsorption on various surfaces; the other was that F^- is a growth inhibitor for the FHAp. Zhu et al. produced rod-like HAp nanoparticles with different aspect ratios in the presence of N-[(2-hydroxy-3-trimethylammonium) propyl] chitosan chloride (HTCC) as a template and by varying reaction conditions, e.g., pH, temperature, and PO_4^{3-}/HTCC ratio [5].

The ordinary hydrothermal method has many weaknesses, for instance, uneven heating and difficulty in obtaining controlled dispersion of HAp. Carrying out the synthesis in an aqueous phase leads to a solid with small particles, which tends to agglomerate into larger aggregates. Hence, their application is limited. To address this issue, we propose a new type of liquid-solid-solution (LSS) assisted hydrothermal method to synthesize monodispersed HAp nanoparticles.

In 2005, Wang et al. [6] proposed a LSS phase transfer strategy to produce multifunctional nanocrystals with different chemical properties. LSS strategy involves an oil-water interface controlled reaction system made of three phases (liquid, solid, and solution) and two interfaces (liquid-solid and solid-solution). In this system, H_2O, C_2H_5OH, RCOOH, and $(RCOO)_nM$ form a three-phase reaction system. The primary solution phase was made up of H_2O and C_2H_5OH in which the precursors of the inorganic salts were dissolved. The solution phase was composed of C_2H_5OH and RCOOH, and the solid phase consisted of $(RCOO)_nM$.

Based on the LSS strategy, Wang et al. [7] synthesized homogeneous HAp nanorods at 80-200°C for about 8-10 h. The obtained samples had tunable size, aspect ratio, and surface properties. Sodium oleate and oleic acid were mixed with C_2H_5OH under stirring. Afterwards, $Ca(NO_3)_2$ was added to form a liquid phase (C_2H_5OH/oleic acid) and a solid phase (sodium oleate). After the exchange between Ca^{2+} and Na^+, calcium dioleate was formed. Finally, Na_3PO_4 was added to the system to react with calcium dioleate. As a result, they successfully obtained HAp nanocrystals highly homogenous in size and narrow size—and length—distributions. To further control the surface properties, they changed the reaction temperature. The results showed that the HAp nanorods had a stable hydrophobic surface at high temperature, since the oleic acid monolayer complexed on the HAp outside surface. Yet, the HAp had an unstable hydrophilic surface because of adsorption of a bilayer of linoleic acid on the HAp surface. Sun et al. [8] synthesized a series of monodisperse HAp doped with selenium based on the LSS strategy. The synthesized pure nanorod HAp was located with the width of around 8 nm and length of around 150 nm. It was noteworthy to find that the width of the obtained nanorods became smaller and the ends of them became sharp compared to pure HAp, though the length of them had no significant change. Huang et al. [9] synthesized HAp nanorods codoped with Eu^{3+} and F^- (FAp:Eu^{3+}) through the LLS strategy to control their size and morphology. The rod-like FAp:Eu^{3+} structures having a smooth surface with diameters of about 15–20 nm and 1engths of about 50–100 nm were obtained. This regular nanostructure makes FAp:Eu^{3+} possess great potential for application in the biomedical fields.

Gemini surfactants are a new type of surfactants, in which two traditional surfactant molecules are connected by a spacer group at the hydrophilic head groups or in close proximity to the head groups. They have advantages over the other monomeric surfactants due to their unique self-assembling ability. We have reported a biomimetic fabrication of HAp with a hollow spherical three-dimensional architecture with polyoxyethylene chain-containing quaternary ammonium salt cationic Gemini surfactant [$C_{12}C_2C_{12}$(EO)] as the template [10].

For reasons dissolved above, in this work, we prepared HAp by the LSS assisted hydrothermal strategy and using a new kind of hyperbranched Gemini quaternary ammonium (PCD) as the template. PCD is a macromolecular cationic surfactant, which has 4 ionic head groups (Figure 1).

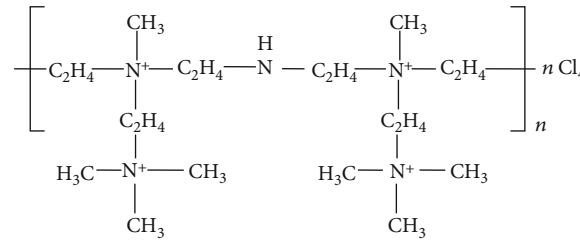

Figure 1: Structure of PCD.

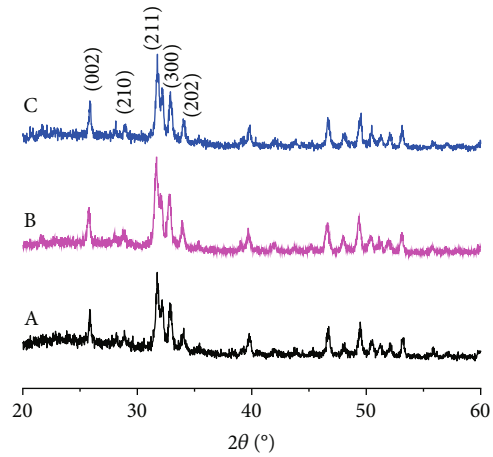

Figure 2: XRD patterns of obtained samples at different conditions. (a) The absence of PCD; (b) 0.005%; (c) 0.05%.

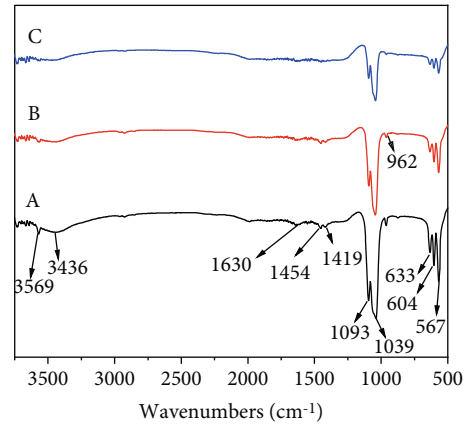

Figure 3: FTIR spectra of samples obtained at different conditions. (a) The absence of PCD; (b) 0.005%; (c) 0.05%.

2. Materials and Methods

2.1. Synthesis of HAp by the Ordinary Hydrothermal Method. In a typical experiment, an appropriate amount of PCD was dissolved in 35 mL 0.17 mol/L $(NH_4)_3PO_4$ solution and magnetically stirred to form solution A. Solution B was made of 35 mL 0.28 mol/L $Ca(NO_3)_2$. Then, solution A was added to solution B under magnetic stirring, and the pH was adjusted to 10.50 with ammonium hydroxide. When the process was finished, stirring was continued for 0.5 h. The reaction product was transferred to a 100 mL autoclave at 180°C for 10 h. The samples were recovered by centrifugation and washed three times with cyclohexane and absolute ethanol, respectively. Finally, the powders were dried at 50°C for 1-2 days.

2.2. Synthesis of HAp by the LSS Strategy. 3.2 g sodium linoleate was dissolved in 8 mL oleic acid under stirring for 2 h. Then, 32 mL C_2H_5OH was added dropwise to the mixed solution under stirring for 15 min to form a suspension. Afterwards, 15 mL 0.28 mol/L $Ca(NO_3)_2$ solution was added to the obtained suspension under stirring. A stable yellow suspension resulted after 1 h under stirring. As a result, a three-phase system made of a liquid phase (C_2H_5OH/oleic

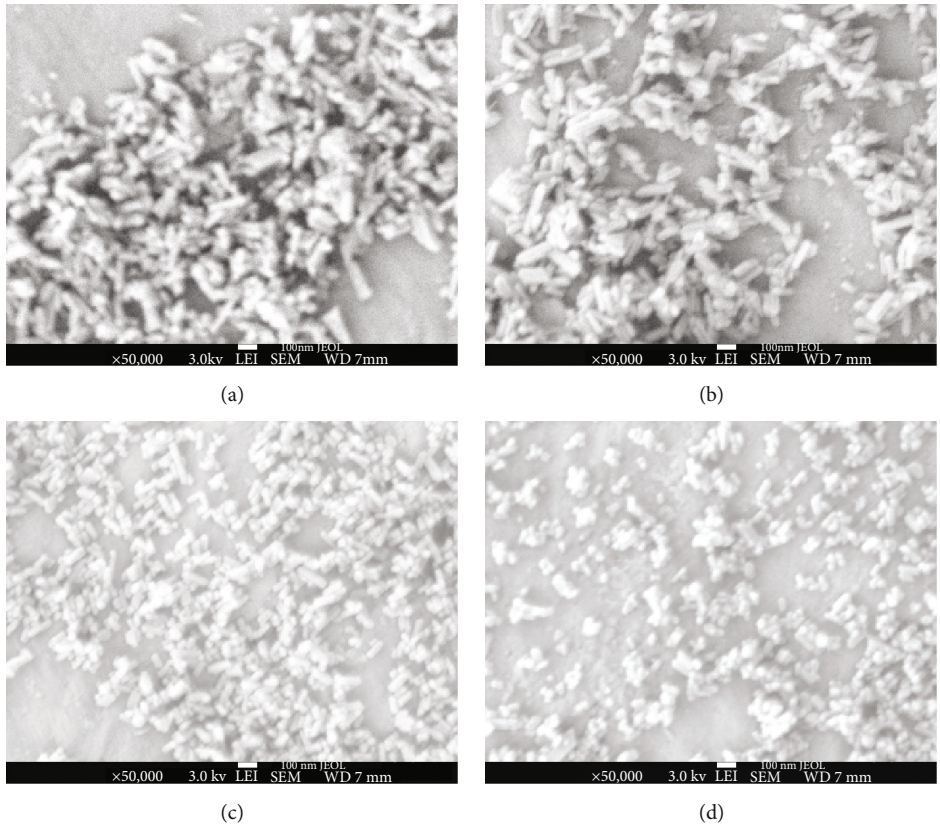

Figure 4: SEM images of obtained samples with different PCD concentrations at 180°C for 10 hours: (a) the absence of PCD; (b) 0.003%; (c) 0.005%; (d) 0.01%.

acid), a solid phase (sodium oleate), and a solution phase ($Ca(NO_3)_2$) was formed. After the exchange between Ca^{2+} and Na^+, calcium dioleate was formed. In the next step, an appropriate amount of PCD was added to 15 mL 0.17 mol/L $(NH_4)_3PO_4$ solution under magnetic stirring for 30 min; then, $(NH_4)_3PO_4$ solution was added to the resulting solution under stirring, and white flocs were formed. The stirring was continued for 5 min. Then, the product was transferred to a 100 mL autoclave at 180°C for 10 h. After cooling to room temperature, the product was centrifuged and washed three times with cyclohexane and absolute ethanol, respectively. Finally, the powders were dried at 50°C for 1-2 days.

2.3. Characterization. The phase of obtained samples was analyzed by X-ray powder diffraction (XRD, Philips X'Pert MPD, Philips Company, Netherlands). The diffraction peak at $2\theta = 25.8°$ was chosen for calculation of the crystallite size because it was sharper and isolated from others which is (002) Miller's plane of the hydroxyapatite crystal. The degree of crystallinity (X_c) was evaluated by using the following equation [11]:

$$X_c = \left(\frac{0.24}{\beta_{002}}\right)^3, \quad (1)$$

where β_{002} is the full width at half maximum (°) of (002) Miller's plane.

The chemical composition of powders was tested by Fourier transform infrared spectroscopy (FT-IR, Nicolet Avatar 360, Thermo-Scientific Ltd., USA). The morphology of particles was studied using a Field Emission Scanning Electron Microscope (FESEM, JEOL 7500F, JEOL Company, Japan). The conductivities of solutions with different PCD concentrations were measured by a conductivity meter (DDS-307A). Based on the conductivity data, a graph was prepared to obtain the cmc value at 37°C, based on the critical turning point.

3. Results and Discussion

3.1. Synthesis of HAp by the Ordinary Hydrothermal Method

3.1.1. The Structural Characterization of Sample. The XRD patterns of HAp in different situations are shown in Figure 2. The XRD peaks at $2\theta = 25.9°$, 31.8°, and 32.9° correspond to the (002), (211), and (300) lattice planes of the HAp phase. Figure 3 illustrates the FTIR spectra of HAp. The band shapes of samples a, b, and c were basically consistent. The bands at 3569 and 633 cm^{-1} correspond to the stretching and twisting vibrations, respectively, of OH groups. The two bands at 3436 and 1630 cm^{-1} were attributed to H_2O adsorbed on the HAp surface. The nonsymmetrical vibration bands at 1093 and 1039 cm^{-1} are assigned to PO_4^{3-} while the bands at 604 and 567 cm^{-1} were attributed to the flexural vibration of PO_4^{3-} [12].

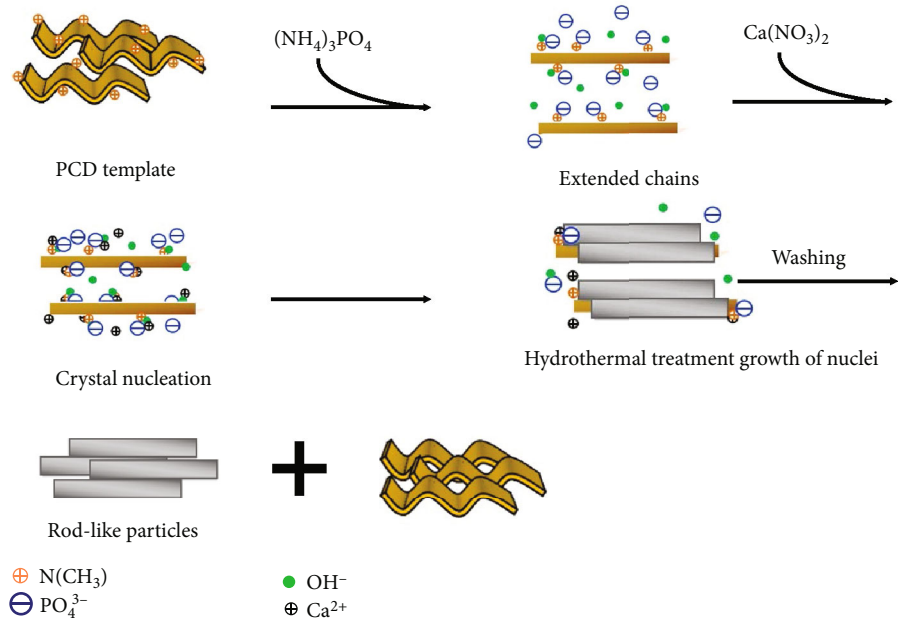

Figure 5: Preparation of rod-like HAp nanoparticles using hydrothermal treatment in the presence of PCD as a Gemini cationic template.

3.1.2. The Morphology of Samples. Figures 4(a)–4(d) depict the SEM images of HAp powders obtained in different reaction systems. The control products display a rod-like structure of different sizes (50-180 nm length, 30-40 nm width). HAp particles are arranged in dens agglomerates. When PCD was used as the template, some changes occurred during the synthesis. On the one hand, the particles are less agglomerated. On the other hand, the length and length/diameter (L/D) ratio are lower. When the PCD was 0.003%, most products were of 180 nm in length and 40-50 nm in width (L/D = 3.6-4.5). When the mass fraction of PCD was 0.005%, the HAp particles were shorter (100 nm in length, 40-50 nm width, L/D = 2-2.5), although a few granular products also existed. Further increasing concentration to 0.01% led to a large number of granular HAp (50 nm length, 40 nm width, L/D = 1.25). In general, the use of PCD resulted in a decrease in the L/D ratio, the shape of solids varying from long rod-like to pellet.

3.1.3. Mechanism of Synthesis. The crystal structure of HAp belongs to the hexagonal system, every unit cell having 10 Ca^{2+}, 6 PO_4^{3-}, and 2 OH^-. When the sample is prepared by the classical hydrothermal treatment, two types of Ca^{2+}-based complexes are formed. One is Ca-P_6O_{24}, which grows along the c-axis, and the other is OH-Ca_6, which grows along the a- and b-axes [13].

As shown in Figure 5, PCD interacts with PO_4^{3-} and OH^- through electrostatic interactions and stereochemical interaction. The macromolecular rigid long chain changed into an extended chain, as a result of the decrease in surface energy. The extended chain interacted with PO_4^{3-} by intermolecular forces to form a 2D structure. Then, the 3D rod-like products were formed by self-assembly of the 2D structure via the hydrogen bonds. Finally, the Ca precursor was added to the system to promote nucleation of the HAp crystals and then their growth during the hydrothermal treatment [5]. At a high concentration of PCD, the concentration of PO_4^{3-}/OH^- is at the interface of organic/water. During the hydrothermal treatment, the HAp crystals grew along the a-, b-, and c- axes. Yet, the growth along the c-axis was inhibited to some extent, resulting in spherical or short rod particles. Since the particles are small, the specific surface area is low and surface energy is higher, which creates favorable conditions for the particles to agglomerate.

Table 1: Electrical conductivity of PCD solution and $(NH_4)_3PO_4$-PCD solution (25°C).

Electrical conductivity ($ms \cdot cm^{-1}$)	C(PCD)/(wt)		
	0.003%	0.01%	0.03%
S_{PCD}	0.05	0.07	0.08
$S_1 = S_{(NH_4)_3PO_4-PCD}$	10.30	10.26	10.20
$S_2 = S_{(NH_4)_3PO_4} + S_{PCD}$	10.38	10.40	10.41
$\Delta S = S_2 - S_1$	0.08	0.14	0.21

To further study the growth process of HAp crystals, an experiment was designed to prove the interaction between PCD and PO_4^{3-}, OH^-, and Ca^{2+}, as shown in Table 1 ($S_{(NH_4)_3PO_4(0.06\,mol/L)} = 10.33\,ms \cdot cm^{-1}$).

When the temperature was constant, several factors, such as the number of ions, ionic charge, and mobility ratio, affected the conductivity of the solution. From the results listed in Table 1, it is evident that increasing the concentration of PCD leads to an increase in S_{PCD}. However, $S_{(NH_4)_3PO_4-PCD}$ was slightly lower than the sum of $S_{(NH_4)_3PO_4}$ and S_{PCD}, namely, $S_{(NH_4)_3PO_4-PCD} \neq S_{(NH_4)_3PO_4} + S_{PCD}$. The

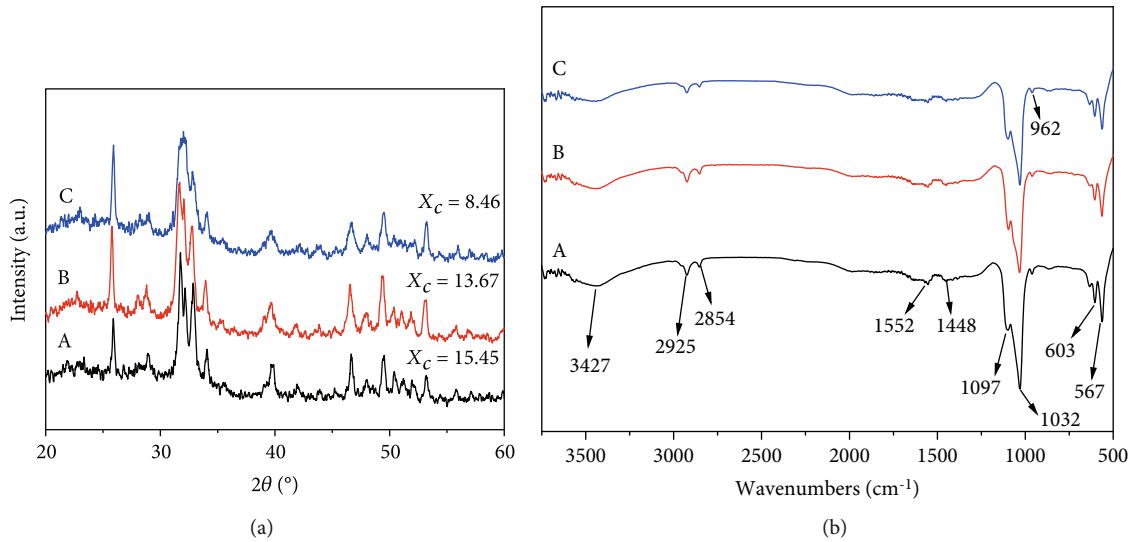

Figure 6: XRD pattern (a) and FTIR spectra (b) of samples obtained with different PCD concentrations at 180°C for 10 hours: (A) the absence of PCD; (B) 0.05%; (C) 0.5%.

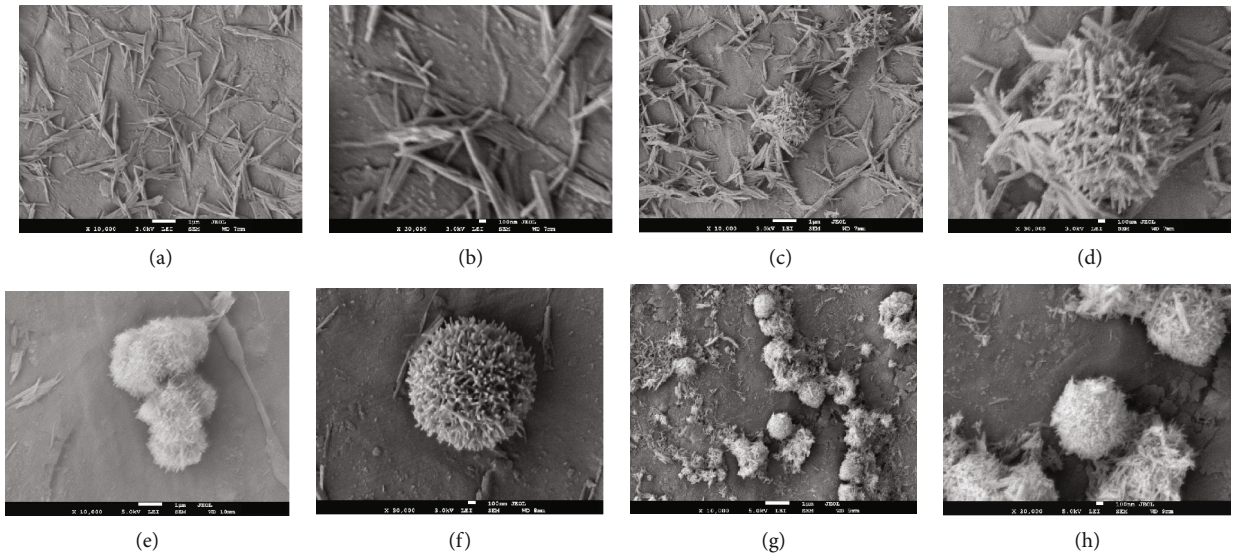

Figure 7: SEM images of obtained samples with different concentrations of PCD at 180°C for 10 h: (a, b) the absence of PCD; (c, d) 0.01%; (e, f) 0.05%; (g, h) 0.5%.

result is explained by the ability of PCD cationic surfactant to attract PO_4^{3-} and OH^- anions, which limited the mobility between PO_4^{3-} and OH^-. As the concentration of PCD increased, the difference between the two values of conductivity gradually increased from 0.08 to 0.21 ms·cm^{-1}. Hence, the intermolecular forces between ions gradually strengthen as the PCD concentration increases.

3.2. Synthesis of HAp in LSS Strategy

3.2.1. The Structural Characterization of Samples. As can be seen from Figure 6, the diffraction peaks of hydroxyapatite obtained at different concentrations of PCD were basically the same. The peak at $2\theta = 32.1°$ became broader and less intense as a result of increasing the concentration of PCD. Therefore, the size and crystallinity of HAp decrease. According to the calculation of crystallinity, the crystallinity (X_c) is 15.45, 13.67, and 8.46, respectively, which decreases with the increase of PCD concentration.

The FTIR spectra depicted in Figure 6 show the characteristic vibration bands of HAp. The absorption peak at 3427 cm^{-1} is due to the vibration of O-H bonds involved in a H bond network with water absorbed on the surface of samples [14]. The bands at 2925 and 2854 cm^{-1} are attributed to the stretch vibration of C-H bonds. The bands at 1097 and 1032 cm^{-1} belong the threefold degenerate antisymmetric stretching vibrations of P-O bond in PO_4^{3-}, whereas the band at 962 cm^{-1} [15] comes from the threefold degenerate symmetric stretching vibration of P-O bond in PO_4^{3-}. The bands at 603 and 567 cm^{-1} are due to the bending vibration of

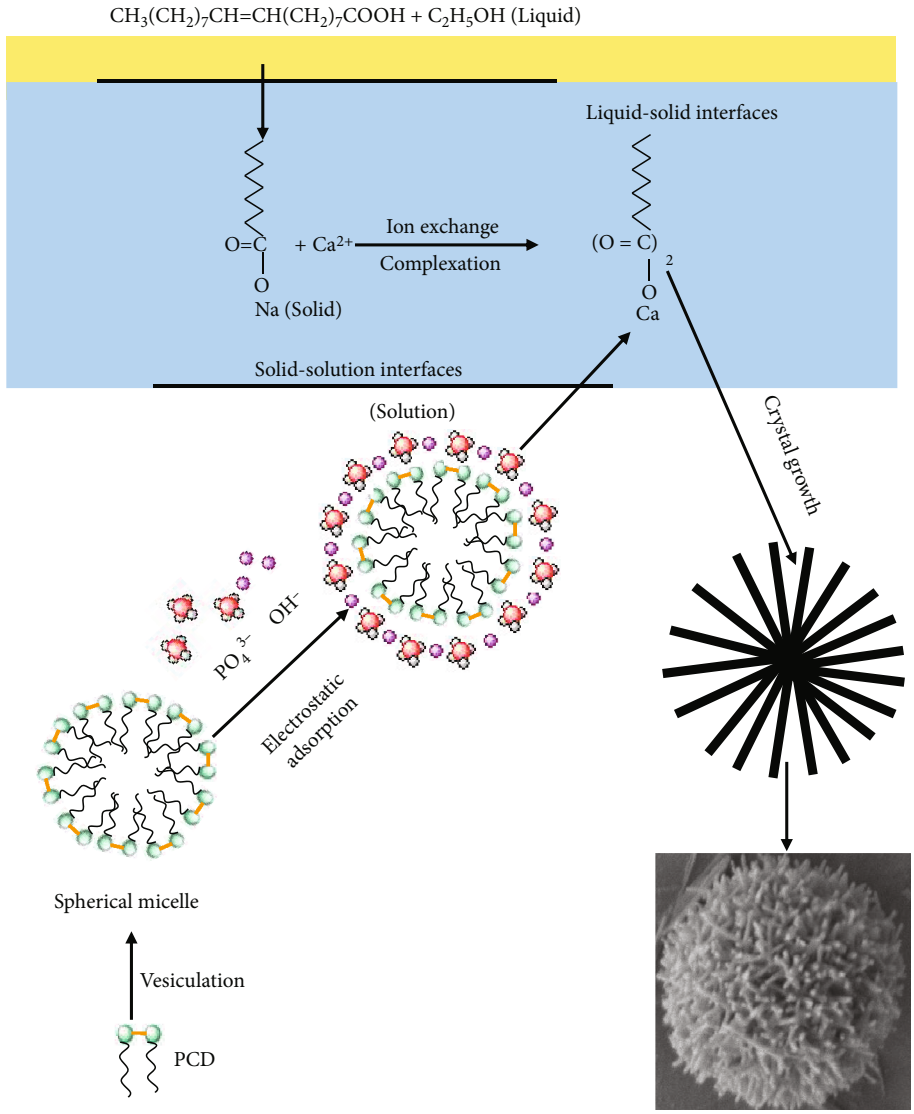

Figure 8: LSS strategy to HAp with Gemini surfactant as template.

PO_4^{3-}. Moreover, two small bands at 1552 and 1448 cm^{-1} appeared in the spectrum and are assigned to the vibration of –O-O- and –COO-, respectively [16].

3.2.2. The Morphology of Samples. Figure 7 displays the morphology and size of HAp particles depending on the concentration of PCD. Figures 7(a) and 7(b) show that the control samples display uniform rods with 0.6-2 μm in length, 25 nm in width, and L/D = 24-80. Because the oleic acid monolayer complexed on the surface and formed a monolayer, HAp has a stable hydrophobic surface. Figures 7(c) and 7(d) show that particles with a near-spherical morphology and size of 1.8 μm were formed when 0.01% PCD was used in the synthesis. Interestingly, when a concentration of 0.05% PCD was used, rods with a length of 0.7 μm gathered into spheres with a diameter of 1.7 μm and homogeneous distribution (Figures 7(e) and 7(f)). Further increase in PCD concentration to 0.5% caused a decrease in size (1.0 μm) of the spherical HAp particles. This was likely due to the fact that the structural unit of HAp crystal decreased to 0.5 μm (Figures 8(g) and 8(h)).

3.2.3. Mechanism of Synthesis. As shown in Figure 8, an ion-exchange reaction occurred between sodium oleate and $Ca(NO_3)_2$ with the formation of calcium dioleate. The PCD cationic surfactant, which can autoassemble in spherical micelles, attracts PO_4^{3-} by electrostatic interactions [17]. Since PCD is hydrophilic and insoluble in oleic acid, the spherical micelles are not damaged. When the phosphate-containing solution is added to calcium dioleate, it immediately attracts calcium dioleate. Rod-like HAp particles grown along the *c*-axis were formed due to the presence of spherical micelle flower-like HAp appearance. The hydrophobicity of HAp was induced by the alkyl chain of oleic acid. We could obtain a mass of HAp at the bottom of the container; the reason was the incompatibility between their hydrophobic surface and polar alcohol. As the PCD concentration increases, crystal growth along *c*-axis is prevented. Hence,

spherical HAp particles made of short rods as structural units were formed.

4. Conclusion

In summary, we prepared rod or sphere HAp particles by the LSS assisted hydrothermal method. The control of shape and size of the HAp particles was achieved by the LSS strategy. More specifically, the morphology, size, and structural organization of HAp particles were well controlled by changing the concentration of the Gemini cationic surfactant during the LSS synthesis. The results revealed the formation of particles of 50-180 nm in length and 30-40 nm in width. Moreover, the reorganization of one-dimensional HAp nanoparticles from one-dimensional into three-dimensional architecture was promoted by this innovative strategy. Therefore, at a concentration of PCD of 0.05%, spherical HAp nanoparticles with narrow size distribution and average size of 1.7 μm were obtained. The difference between them was due to the shape of the micelles in the solution. The former had rod-like shape while the latter had spherical shape.

Data Availability

The data used to support the findings of this study are available from the corresponding author upon request.

Conflicts of Interest

The authors declare that there is no conflict of interest regarding the publication of this paper.

Acknowledgments

The authors gratefully acknowledge the financial support of the Natural Science Foundation of Fujian Province (Nos. 2016J01595 and 2019J01546), the Project of innovation platform for Fuzhou Health and Family Planning Commission (Nos. 2017-S-wp1 and 2018-S-wp3), the Key Clinical Specialty Discipline Construction Program of Fujian Province, the Major Science and Technology Projects of Fuzhou (2017), and the Project of Fuzhou Health and Family Planning Youth Scientific (2018-S-wq10).

References

[1] P. T. Kien, H. D. Phu, N. V. V. Linh, T. N. Quyen, and N. T. Hoa, "Recent trends in hydroxyapatite (HA) synthesis and the synthesis report of nanostructure HA by hydrothermal reaction," in *Novel Biomaterials for Regenerative Medicine*, vol. 1077, pp. 343–354, Springer, Singapore, 2018.

[2] H. Zhang and M. Zhang, "Characterization and thermal behavior of calcium deficient hydroxyapatite whiskers with various Ca/P ratios," *Materials Chemistry and Physics*, vol. 126, no. 3, pp. 642–648, 2011.

[3] H. Zhang and M. Zhang, "Phase and thermal stability of hydroxyapatite whiskers precipitated using amine additives," *Cereal Chemistry*, vol. 37, no. 1, pp. 279–286, 2011.

[4] D. Jiang, D. Li, J. Xie et al., "Shape-controlled synthesis of F-substituted hydroxyapatite microcrystals in the presence of Na_2EDTA and citric acid," *Journal of Colloid and Interface Science*, vol. 350, no. 1, pp. 30–38, 2010.

[5] A. Zhu, Y. Lu, Y. Si, and S. Dai, "Frabicating hydroxyapatite nanorods using a biomacromolecule template," *Applied Surface Science*, vol. 257, no. 8, pp. 3174–3179, 2011.

[6] X. Wang, J. Zhuang, Q. Peng, and Y. Li, "A general strategy for nanocrystal synthesis," *Nature*, vol. 437, no. 7055, pp. 121–124, 2005.

[7] X. Wang, J. Zhuang, Q. Peng, and Y. D. Li, "Liquid-solid-solution synthesis of biomedical hydroxyapatite nanorods," *Advanced Materials*, vol. 18, no. 15, pp. 2031–2034, 2006.

[8] J. P. Sun, X. Y. Zheng, H. Li et al., "Monodisperse selenium-substituted hydroxyapatite: controllable synthesis and biocompatibility," *Materials Science and Engineering: C*, vol. 73, pp. 596–602, 2017.

[9] L. Huang, W. H. Luo, M. Y. Liu et al., "Facile preparation of Eu^{3+} and F^{-} co-doped luminescent hydroxyapatite polymer composites _via_ the photo-RAFT polymerization," *Journal of the Taiwan Institute of Chemical Engineers*, vol. 83, pp. 184–191, 2018.

[10] T. Zhang, G. P. Chen, Y. Y. Zhang, and X. F. Xiao, "Biomimetic fabrication of hydroxyapatite hollow spheres with polyoxyethylene chain-containing quaternary ammonium salt cationic Gemini surfactant as template," *Soft Materials*, vol. 17, no. 2, pp. 159–169, 2019.

[11] G. S. Kumar, A. Thamizhavel, Y. Yokogawa, S. N. Kalkura, and E. K. Girija, "Synthesis, characterization and *in vitro* studies of zinc and carbonate co- substituted nano-hydroxyapatite for biomedical applications," *Materials Chemistry and Physics*, vol. 134, no. 2-3, pp. 1127–1135, 2012.

[12] X. F. Xiao, R. F. Liu, F. Liu, X. Zheng, and D. C. Zhu, "Effect of poly(sodium 4-styrene-sulfonate) on the crystal growth of hydroxyapatite prepared by hydrothermal method," *Materials Chemistry and Physics*, vol. 120, no. 2-3, pp. 603–607, 2010.

[13] M. L. Qi, K. He, Z. N. Huang et al., "Hydroxyapatite fibers: a review of synthesis methods," *JOM*, vol. 69, no. 8, pp. 1354–1360, 2017.

[14] K. Lin, J. Chang, Y. Zhu et al., "A facile one-step surfactant-free and low-temperature hydrothermal method to prepare uniform 3D structured carbonated apatite flowers," *Crystal Growth & Design*, vol. 9, no. 1, pp. 177–181, 2009.

[15] H. Nishikawa, D. Okumura, and M. Kusunoki, *Application of Hydroxyapatite Thin Film as a Biosensor*, American Physical Society, APS March Meeting, 2006.

[16] J. Hui and X. Wang, "Hydroxyapatite nanocrystals: colloidal chemistry, assembly and their biological applications," *Inorganic Chemistry Frontiers*, vol. 1, no. 3, pp. 215–225, 2014.

[17] Z. Y. Du, Y. You, R. Jiang et al., "Synthesis of sodium carboxylate Gemini surfactants containing a p-phendioxy spacer and their micellization in aqueous solution," *Chemical Research in Chinese Universities*, vol. 11, pp. 2056–2059, 2003.